Available online at www.sciencedirect.com

SciVerse ScienceDirect

Ceramics International 39 (2013) 7483–7490

CERAMICS INTERNATIONAL

www.elsevier.com/locate/ceramint

Efficient optimum solution for high strength Al alloys matrix composites

Ali Asghar Tofigh, Mohsen Ostad Shabani*

Materials and Energy Research Center (MERC), Tehran, Iran

Received 8 November 2012; received in revised form 23 February 2013; accepted 28 February 2013
Available online 14 March 2013

Abstract

This papers describes a search technique to optimize the fabrication process conditions of the high wear resistance Al alloy matrix composites reinforced with different volume percentages of boron carbide particles. An experimental investigation was then carried out on the abrasive wear behavior of the composites in terms of abrasive particle size, weight fraction and applied load in pin-on-disc type of wear machine. Particle swarm optimization suffers from premature convergence problems when applied to high-dimensional problems, which results in a low optimization precision or even failure. In this study, a self-organizing hierarchical particle swarm optimizer based on the shrinking strategy is introduced for high dimensional function processing optimization of Al matrix composites in order to avoid the premature convergence effectively.

Keywords: Aluminum; B_4C; Wear

1. Introduction

There has been an upsurge of using Al alloys in many automobile, aerospace and mineral processing components due to their excellent combination of low density, high thermal conductivity and high strength-to-weight ratio [1–8]. In recent times, attention is especially being paid to the use of high strength Al alloys for structural applications in aerospace and general engineering sectors [9,10]. However, these materials are of poor weldability. Thus, most of these materials are joined either by riveting or bolting, and hence there is a greater possibility of vibration/oscillation in these regions, which in due course might lead to fretting and sliding types of wear in dry conditions [11–20]. Aluminum matrix composites reinforced with hard ceramic particles have emerged as a potential material, especially for wear resistant applications such as brake drums, cylinder liners, pistons, cylinder blocks, connecting rods, etc. [8–10]. Among the reinforcements, such as B_4C, SiC, TiC, B, C and Al_2O_3, B_4C is most widely used due to its low cost, wide range of available grades, higher stability and chemical compatibility with Al matrix [21–28]. Fabrication of high wear resistance Aluminum matrix composites reinforced with B_4C particles demands the need to optimize the fabrication process conditions and experimentally examine the dry sling wear behavior of optimized composite systems [29–31].

There has been extensive research attention in function optimization. In order to solve a wide range of complex optimization problems, a number of machine learning techniques such as neural networks, evolutionary algorithms, and swarm intelligence-based algorithms, are developed and applied successfully [32–35]. This research is mostly focused on developing algorithms that can locate only a single solution. However, evolutionary algorithms research has produced a number of approaches to find multiple solutions. Particle swarm optimizers (PSO) are optimization algorithms modeled after the social behavior of birds in a flock [36–38]. PSO is a population based search process where individuals, referred to as particles, are grouped into a swarm [36]. Each particle in a swarm represents a candidate solution to the optimization problem. In a PSO system, each particle is flown through the multidimensional search space, adjusting its position in search space according to its own experience

*Corresponding author. Tel.: +98 912 563 6709; fax: +98 261 6201888.
E-mail addresses: vahid_ostadshabany@yahoo.com, m-ostadshabany@merc.ac.ir (M.O. Shabani).

0272-8842/$ - see front matter © 2013 Elsevier Ltd and Techna Group S.r.l. All rights reserved.
http://dx.doi.org/10.1016/j.ceramint.2013.02.097

and that of neighboring particles. A particle therefore makes use of the best position encountered by itself and that of its neighbors to position itself toward an optimal solution [39–42]. The effect is that particles "fly" toward a minimum, while still searching a wide area around the best solution. The performance of each particle (i.e., the "closeness" of a particle to the global optimum) is measured using a pre-defined fitness function which encapsulates the characteristics of the optimization problem.

Since the publication of PSO in 1995, there has been a considerable amount of work done in developing the original version of PSO, through empirical simulations, integration of its self-adaptation, parameter selecting, swarm topology and integrating with other intelligent optimizing methods [40–44]. Proper control of global exploration and local exploitation is crucial in finding the optimum solution efficiently. The concept of inertia weight to the original version of PSO is introduced, in order to balance the local and global search during the optimization process. The concept of time-varying acceleration coefficients is proposed to effectively control the global search and convergence to the global best solution [34]. The major consideration of this modification is to avoid premature convergence in the early stages of the search and to enhance convergence to the global optimum solution during the latter stages of the search [41]. In PSO, lack of diversity of the population, particularly during the latter stages of the optimization, was understood to be the dominant factor for the convergence of particles to local optimum solutions prematurely. Recently, several attempts on improving the diversity of the population have been reported [45–47]. A "mutation" operator is introduced to the particle swarm concept by considering the behavior of the particles during the search. Under this new strategy, when the global optimum solution does not improve with the increasing number of generations, a particle is selected randomly and then a random perturbation is added to a randomly selected modulus of the velocity vector of that particle. It is suggested that for complex multimodal functions, the control of diversity of the population with a linearly varying inertia weight may lead the particles to converge to a local optimum prematurely [48]. On the other hand, it is shown that the constriction factor method is ineffective for complex multimodal functions, despite its ability to converge to stopping criteria at a significantly faster rate for unimodal functions [37]. Based on these results, a self-organizing hierarchical particle swarm optimizer is introduced. Under this method, the previous velocity term is kept constant at zero. The momentum for the particles to roam through the search space is maintained by re-initializing particles with random velocities, whenever they stagnate in the search space [48–54]. This method kept the previous velocity term at zero, and reinitialized the modulus of velocity vector of a particle with a random velocity when it stagnates in the search space. Therefore, a series of particle swarm optimizers are automatically generated inside the main particle swarm optimizer according to the behavior of the particles in the search space, until the convergence criteria is met. In view of this, attempts are made to successfully apply this method, in order to optimize the fabrication process conditions of aluminum and AMCs.

2. Experimental procedure

Al alloy matrix composites including various volume fractions of B_4C particles with average particle sizes of 1, 10, 21, 33 and 55 μm were produced by liquid metallurgy method. The chemical composition of aluminum alloy and B_4C are represented in Tables 1 and 2, respectively. Boron carbide is an attractive ceramic reinforcement for a range of application including wear components, mechanical seals, aerospace parts and cutting tools Further, its density ($2.52\ g\ cm^{-3}$) is very close to the Al alloy matrix. However, in terms of preparing Al–B_4C composites, especially with a high B_4C content, the wettability of particles represents a very important issue, which is poor at temperatures near the melting point of aluminum (660 °C). Thus, attention was paid to the fact that B_4C powders coated with some Ti compounds might have reasonable wettability with aluminum. The sol–gel technique was implemented in order to coat the B_4C particles with TiB_2.

The aluminum ingot was placed in a graphite crucible and heated to above the alloy liquidus temperature using the resistance furnace. Argon gas was also blown into the crucible during the operation. After the entire alloy in the crucible was melted, the impeller was turned on and set to the pre-determined speed (600 rev/min). Then 5, 10, 15, 20, 25 and 30 vol% B_4C particles, which were heated at 400 °C for 10 min and air-cooled to room temperature (about 25 °C) before incorporation, were added into the uniformly formed vortex. The molten mixture was step cast into the CO_2–sand mold. Unreinforced Al matrix alloy sample was also produced by the same method.

Table 1
Chemical composition of Aluminum matrix composites.

Element	Wt%
Zn	5.91
Mg	1.61
Fe	0.31
Cu	0.01
Al	Balance

Table 2
Chemical composition of B_4C.

Total Boron	77.5%
Total Carbon	21.5%
Total Iron	0.2%
Total B+C	**98**%

The experimental density of the composites was obtained by the Archimedian method of weighing small pieces cut from the composite cylinder first in air and then in water, while the theoretical density was calculated using the mixture rule according to the weight fraction of the particles. The porosities of the produced composites were evaluated from the difference between the expected and the observed density of each sample.

A pin-on-disc type of apparatus was employed to evaluate the wear characteristics of MMCs. A systematic view of the testing machine is shown in Fig. 1. The specimen surfaces were ground well prior to initiating the wear tests and subjected to few runs against the counter surface at slow speed and low load for establishing intimate contact between the two matting surfaces. The slider disc was case hardened steel with 63 HRC to a depth of 3 mm. Test specimens were cut and shaped in the form of pins having 6 mm diameter and 25 mm height. The disc surface is regularly and thoroughly cleaned by acetone prior to and after wear testing. The wear pin was cleaned in acetone prior to and after the wear tests, dried, and after that weighed on a micro-balance with 0.1 mg sensitiveness.

3. Modeling

Artificial neural networks is a branch of modern information technology which is increasingly being applied to engineering fields in order to solve various complex problems. Based on the given input and output, a model can be constructed very easily and trained to predict process dynamics accurately [36]. All artificial neural networks are basically analogous in topological structure. Some of the neurons interface with the real world to receive its input, and other neurons provide the real world with the network's output. All the rest of the neurons are hidden from view. The interconnections between neurons determine the network function, which are not simple [39]. Each input to a neuron has a weight factor of the function that determines the strength of the interconnection, and thus the contribution of that interconnection to the following neurons [42]. ANNs can be trained to perform a particular function by adjusting the values of these weight factors between the neurons, either from the information from outside the network or by the neurons themselves in response to the input. This is the key to the ability of ANNs to achieve learning and memory. The characteristics of most suitable applications for ANNs include an available large database, difficulty in finding an accurate solution to the problem by existing mathematical approaches and the incomplete, noisy or complex dataset. However, the limitations of the ANN method are such as essential close relationship between Training data of the database with the predicting parameters and necessity of sufficient training data. In addition, even though well trained ANNs may contribute to the development of a mechanistic understanding of the considered problem, ANNs are purely phenomenological and does not inherently produce a mechanistic understanding of the process being modeled [44]. FEM was used for discretization. Fig. 2 shows the flowchart of the combined FEM–PSO–ANN model which has been used in this investigation. In order to find an optimal architecture, different numbers of neurons in the hidden layer were considered and root mean square (RMS) error for each network was calculated. The network developed in this study, consists of four input nodes namely cooling rate, temperature gradient, volume percentage and average particle size of B_4C, and the two output parameters namely variation of porosity and weight loss. For experiments in this paper, the total error, was used as a criterion for terminating the training session. The numbers of neurons in hidden layer are determined by trial and error during training. The effect of numbers of neurons in the hidden layer on the network performance is shown in Fig. 3. It is clear the optimum number of neurons that gives the minimum error in the hidden layer is 10, and could be used as a fitness function in modified particle swarm optimization.

3.1. Optimization

Optimization problems can be broadly categorized into unimodal and multi-modal problems. Function optimization is the process of finding an optimal solution to an objective function describing a problem [38]. Optimization can be either a minimization or maximization task. Like

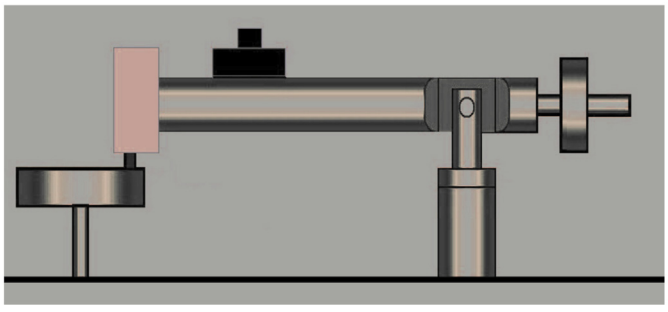

Fig. 1. Schematic diagram of the abrasion wear test.

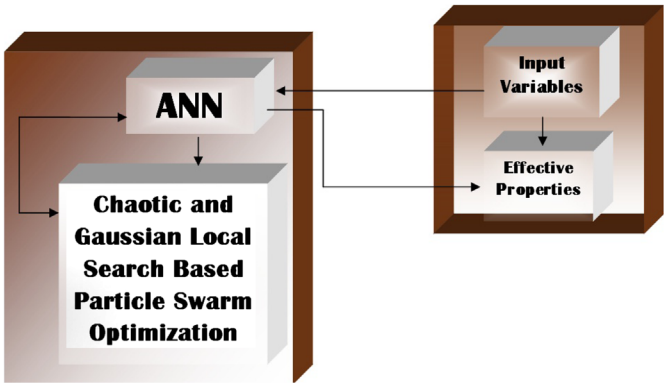

Fig. 2. Flowchart of combined FEM–PSO–ANN model.

other population based optimization algorithms, PSO has two phases: initialization and evolution. In the initialization phase, the population is initialized with uniformly distributed random particles within their search space [42]. In the evolution phase, particles search for the optima by updating themselves based on their current and historic information until termination criteria is met. In the original PSO with M particles, each particle is represented as a potential solution to a problem in a D-dimensional space and its position at the tth iteration is denoted as

$$X_i = (x_{i1}{}^t, x_{i2}{}^t \ldots x_{iD}{}^t) \quad (1)$$

Each particle remembers its own previous best position and its velocity along each dimension as

$$V_i = (v_{i1}{}^t,\ v_{i2}{}^t \ldots v_{iD}{}^t) \quad (2)$$

The velocity and position of particle i at the $(t+1)$th iteration are updated by the following equations:

$$V_{i,j}^{t+1} = wV_{i,j}^t + c_1 r_{1i,j}^t (p_{ij}^t - x_{ij}^t) + c_2 r_{2i,j}^t (Q_j^t - X_{i,j}^t) \quad (3)$$

$$X_{i,j}^{t+1} = V_{i,j}^{t+1} + X_{i,j}^t \quad (4)$$

where c_1 and c_2 are two positive constants, known as the acceleration coefficients; and r_1 and r_2 are two uniformly distributed random numbers in the range (0,1) for the jth dimension of particle i. Vector $p_i=(p_{i1}^t,\ p_{i2}^t \ldots\ p_{iD}^t)$ is the position with the best fitness found so far for the ith particle, which is called the personal best (p_{best}) position, and vector $Q_i=(Q_1^t,\ p_2^t \ldots\ p_D^t)$ records the best position discovered by the swarm so far, known as the global best (g_{best}) position. $xi_{,j}^t$, $v_{i,j}^t$ and $p_{i,j}^t$ are the jth dimension of vector of x_i^t, v_i^t and p_i^t, respectively [45–47,48]. The parameter w is the inertia weight used for the balance between the global and local search abilities. Usually, w decreases linearly with the iteration generations as

$$w = w_{\max} - t \times (w_{\max} - w_{\min})/T \quad (5)$$

where $w_{\max}$ and $w_{\min}$ are the maximum and minimum weights, usually set to 0.9 and 0.4, respectively. T is a predefined maximum number of iterations, and t represents the number of current iterations [42–47]. Let f be the objective function to be minimized. The PSO algorithm can be described by the following pseudocode.

In this paper, a Logistic Chaotic map is employed.

$$\beta_j^{k+1} = \mu\beta_j^k(1-\beta_j^k) \quad (6)$$

Where β_j is the jth Chaotic variable in the kth generation. When $\mu=4$, the Logistic function comes into a thorough chaos state. To further enhance the performance of the PSO, in this paper a Chaotic and Gaussian local search based on the "shrinking" strategy is used, expressed by

$$X_i^{'g} = X_i^g(1-\lambda) + \lambda\beta_c \quad (7)$$

where $X_i^{g\prime}$ is a new vector related to particle X_i^g in the gth generation produced by Chaotic or Gaussian local search, β_c is a Chaotic or Gaussian vector generated by Chaotic or Gaussian iteration and then mapped into the search space, and λ is the "shrinking" scale, given by

$$\lambda = 1 - \left|\frac{\text{FEs-1}}{\text{FEs}}\right|^m \quad (8)$$

Where FEs is the current function evaluation numbers, m controls the "shrinking" speed and is set to Max_FEs/5. The maximum allowed local iteration number is set to 100. If $X_i^{g\prime}$ is better than X_i^g; X_i^g is replaced by $X_i^{g\prime}$ and the local search iteration stops immediately to save the function evaluations [43–47].

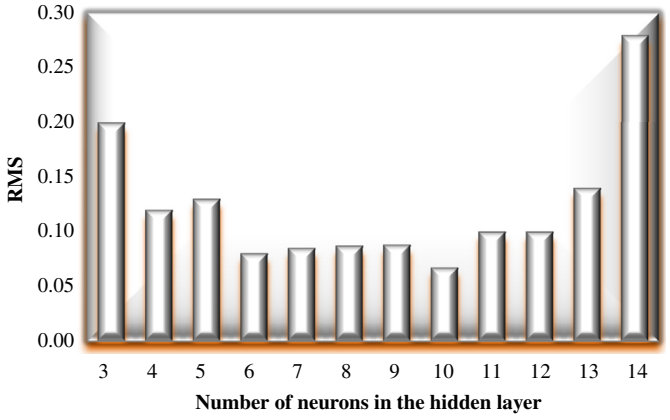

Fig. 3. Effect of numbers of neurons in the hidden layer on the network performance.

4. Results and discussion

Abrasive wear occurs when hard particles or asperities penetrate a softer surface and displace material in the form of elongated chips and slivers. Wear resistance is not an

Table 3
Wear loss as a function of sliding distance.

Sliding distance (m)	Weight loss (mg) for unreinforced	Weight loss (mg) for 5%	Weight loss (mg) for 10%	Weight loss (mg) for 15%	Weight loss (mg) for 20%	Weight loss (mg) for 25%	Weight loss (mg) for 30%
0	0	0	0	0	0	0	0
200	1.01	0.81	0.52	0.43	0.34	0.24	0.19
400	1.53	1.22	1.23	0.72	0.52	0.34	0.25
600	1.74	1.62	1.41	0.93	0.63	0.44	0.35
800	2.13	1.83	1.62	1.11	0.84	0.67	0.52
1000	2.42	2.11	1.91	1.32	0.91	0.79	0.67

intrinsic property of a material, but depends upon the tribological system, such as properties of materials tested, microstructure and interface, abrasive grit size, test condition, equipment and environment [9]. Table 3 shows the wear resistance of the composites and matrix alloy. It is noted that the weight loss of the composites and the matrix alloy increases with increasing the sliding distance. In general, composites offer superior wear resistance as compared to the alloy irrespective of applied pressure and sliding speed. This is primarily due to the fact that the hard dispersoid makes the matrix alloy plastically constrained and improves the high temperature strength of the virgin alloy [5]. Additionally, the hard dispersoids, present on the surface of the composite as protrusions, protect the matrix from severe contact with the counter surfaces [7], and thus results in less wear, a lower coefficient of friction and temperature rise in composites as compared to those in the alloy [5]. Unreinforced Al alloy exhibits an extremely high weight loss during abrasive sliding, as expected. In the case of composites, the B_4C particles remain intact during wear in order to support the applied load and act as effective abrasive elements. The particles protruding from the surface of the composite bear most of the wear load, and the surface hardness of the composite is mainly a result of the hardness of the particles.

Several investigators have reported a critical applied load above which composites suffer from either equal or higher wear rate with respect to that of the alloy under similar tribo conditions. They observed that this is happening due to fracture, fragmentation and removal of ceramic fiber or particles which ultimately leads to delaminating type of wear. Additional drawback of composites with hard rigid ceramic reinforcements is the tendency of these phases to act as rigid abrasive particles, which are causing more abrasive action to the counter surface. Furthermore, liberated reinforcing particles as wear debris roll over the contacting surfaces which creates three body abrasion type situation and causing more wear on both the contacting surface. However, the extent of this situation depends on sliding speed, applied load and frictional heating. In fact, during sliding wear of metals and alloys, a mechanically mixed layer (MML) is formed over the specimen surface, which strongly dictates the wear behavior of the materials. It is believed that these layers are formed due to formation of wear debris, transfer of materials from the counter surfaces, mixing and compaction of these materials on the contact surfaces under applied load and higher frictional heating.

The unreinforced matrix alloy was much softer than the slider, therefore the slider penetrate and cut deeply into the surface, which causes extensive plastic deformation of the surface and consequently a great amount of material loss. A typical SEM micrograph of the worn surfaces of the Al alloy is shown in Fig. 4(a). The worn surface of the unreinforced Al matrix alloy was characterized by extensive plastic deformation and obvious evidence of plowing, cutting and smearing. Mainly, a three-body rolling wear mechanism characterized bymultiple indentations and very short plowing or cutting grooves was seen. For the investigated composites, the most important feature is the presence of B_4C particles, the hardness of which is much higher than that of the matrix alloy. The typical worn surface of the composites is shown in Fig. 4(b). The B_4C particles strengthen the aluminum matrix and protect the softer matrix during abrasive wear. The worn surfaces of the composites were somewhat analogous to that of the unreinforced matrix alloy and were characterized by mainly plastic deformation, with some plowing and cutting effects.

Irrespective of attempts to optimize the fabrication parameters, there exist some defects including porosity, which is very difficult to overcome in cast composites.

The variation of porosity with the B_4C content is shown in Table 4. Increasing amount of porosity is observed with increasing the volume fraction. The porosity is normal, because of the long particle feeding duration and the increase in surface area in contact with air caused by increasing the

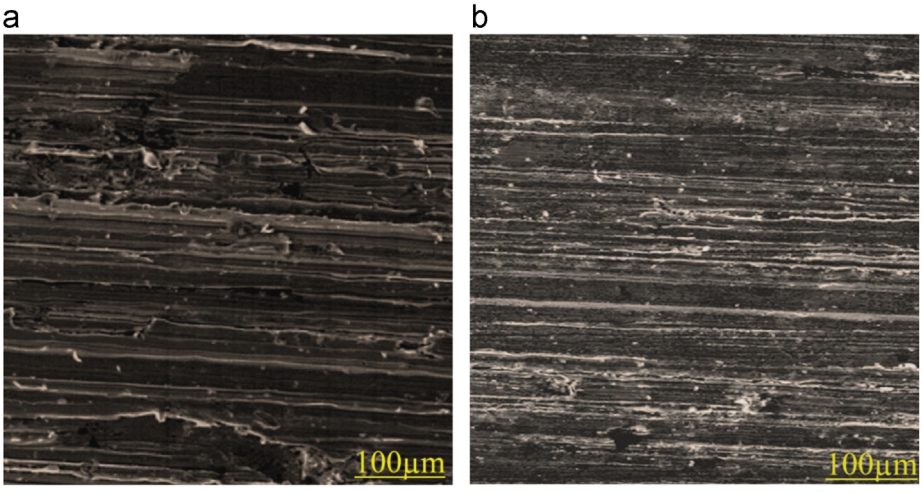

Fig. 4. Typical worn surface of the unreinforced Al alloy (a) and composites (b).

Table 4
Variations of porosity of the composites.

Volume % B_4C	Volume % porosity (55 μm)	Volume % porosity (33 μm)	Volume % porosity (21 μm)	Volume % porosity (10 μm)	Volume % porosity (1 μm)
0	0.7	0.7	0.7	0.7	0.7
5	1	1.2	1.5	1.8	2.3
10	1.3	1.5	1.9	2.2	2.7
15	1.7	2	2.3	2.6	3.1
20	2	2.3	2.7	3	3.5
25	2.3	2.7	3.1	3.4	3.9
30	2.7	3.1	3.5	3.8	4.1

particle content. This trend is also reported by the early works [9]. It is shown that for the fixed B_4C particles content, the porosity of composite samples decrease with the coating of B_4C particles. This is attributed to porosity associated with the particle clusters and hindered liquid metal flow.

5. Modeling results

With the "shrinking" strategy, the local search space is decreased linearly throughout the run process around the optimum obtained so far. Combining PSO with Chaotic and Gaussian local searches, a new PSO algorithm can be constructed. Considering the effectiveness, only the global best particle from the whole swarm carries out the Chaotic or Gaussian local search in every generation. The procedure of new PSO is:

Step 1. Initialization.
Step 2. Initialize the population size PopSize, inertia weight w, acceleration factors c_1 and c_2, as well as maximum allowed function evaluations Max_FEs.
Step 3. Initialize all particles X_i^0 and V_i^0.
Step 4. Evaluate X_i over all particles.
Step 5. Identify the p_{best} for each particle and g_{best} for all particles.
Step 6. Iteration.
Step 7. Update the velocity V_i^q according to Eq. (3).
Step 8. Update the position X_i^q according to Eq. (4).
Step 9. Update the p_{best} and g_{best}.
Step 10. Implement Chaotic or Gaussian local search with the "shrinking" strategy on the g_{best} particle.
Step 11. If the stopping criterion is met, output the best solution g_{best} found so far. Otherwise, jump to Step 6.

Final optimized Al matrix composites process parameters are 19.24 vol% of B_4C, 2.13 vol% of porosity and 0.97 mg weight loss. Therefore, PSO gives the optimal process conditions of Al matrix reinforced with B_4C particulates. In this new proposed PSO, better optimization results are achieved and compared to those of general PSO by splitting the cognitive component of the general PSO into two different components. The first component can be called good experience component. This means the bird has a memory about its previously visited best position. This is similar to the general PSO method. The second component is given the name bad experience component. The bad experience component helps the particle to remember its previously visited worst positions. To calculate the new velocity, the bad experiences of the particles are also taken into consideration. In the early run phase, Chaotic local search is employed to explore a large search space to avoid premature convergence, and in the late run phase, Gaussian local search is used to exploit a small search space around the optimum to further refine the outputs. The effectiveness of the Chaotic and Gaussian local search on improving the standard PSO was demonstrated using a fair comparison over 13 scalable benchmark functions. The acceleration factors c_1 and c_2 were set at 1.5 and population size was set at 125. When the current function evaluation reached 80% of the maximum FEs, the Chaos local search strategy was switched to the Gaussian local search strategy. RMS error is used to evaluate the forecasting accuracy; Fig. 5 shows the effect of iteration number on the RMS of developed model.

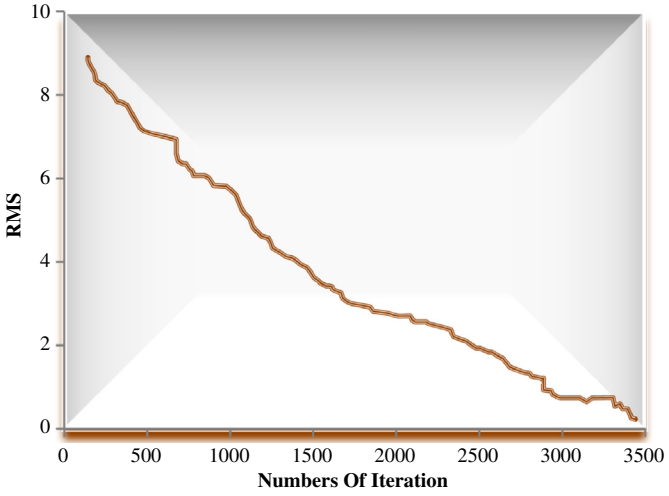

Fig. 5. Effect of iteration number on the RMS.

6. Conclusion

In this paper, a novel search technique is successfully used to optimize the fabrication process conditions of the high wear resistance Al alloy matrix composites, which combine Chaotic and Gaussian local searches based on the shrinking strategy. A series of particle swarm optimizers are automatically generated inside the main particle swarm optimizer according to the behavior of the particles in the search space, until the convergence criteria is met. It is concluded that this technique helps to avoid premature convergence problems, and thus can be applied to high-dimensional problems. Experimental investigation shows that the wear resistance of the alloy is improved significantly due to particle addition. The composite exhibited a lower wear rate than that of the matrix alloy. Further, the wear rate of composite decreased with increase in B_4C concentration. The surface roughness of the composites decreases

with increasing B_4C particle size. Since the particle–matrix interfacial area was larger in the case of a small particle size the chance for the small particles of B_4C to escape from the matrix alloy increases. Large particles of B_4C are expected to remain inside the surface for a long time until they wear out and break down into smaller particles; consequently, the composites with large B_4C particle size show a better wear resistance during abrasive wear.

References

[1] S.S. Byeon, K. Wang, Y.J. Seo, Y.G. Jung, B.H. Koo, Structural properties of the oxide coatings prepared by electrolyte plasma process on the Al 2021 alloy in various nitrogen solutions, Ceramics International 38 (2012) S665–S668.

[2] Y.M. Wang, H. Tian, X.E. Shen, L. Wen, J.H. Ouyang, Y. Zhou, D.C. Jia, L.X. Guo, An elevated temperature infrared emissivity ceramic coating formed on 2024 aluminum alloy by microarc oxidation, Ceramics International 39 (3) (2013) 2869–2875.

[3] M.O. Shabani, A. Mazahery, The synthesis of the particulates Al matrix composites by the compocasting method, Ceramics International 39 (2013) 1351–1358.

[4] R. Bauri, M.K. Surappa, Processing and compressive strength of Al–Li–SiCp composites fabricated by compound billet technique, Journal of Material Processing Technology 209 (2009) 2077–2084.

[5] M.O. Shabani, A. Mazahery, Optimization of process conditions in casting aluminum matrix composites via interconnection of artificial neurons and progressive solutions, Ceramics International 38 (2012) 4541–4547.

[6] J. Hashim, L. Looney, M.S.J. Hashmi, Particle distribution in cast metal matrix composites. Part I, Journal of Materials Processing Technology 123 (2002) 251–257.

[7] A. Mazahery, M.O. Shabani, Tribological behavior of semisolid–semisolid compocast Al–Si matrix composites reinforced with TiB_2 coated B_4C particulates, Ceramics International 38 (2012) 1887–1895.

[8] W.R. Blumenthal, G.T. Gray, T.N. Claytor, Response of aluminum-infiltrated boron carbide cermets to shock wave loading, Journal of Materials Science 29 (1994) 4567.

[9] M.O. Shabani, A. Mazahery, The performance of various artificial neurons interconnections in the modelling and experimental manufacturing of the composites, Materiali in Tehnologije 46 (2) (2012) 109–113.

[10] A.J. Pyzik, I.A. Aksay, Processing of ceramic and metal matrix composites, in: Proceedings of the International Symposium on Advances in Processing of Ceramic and Metal Matrix Composites, New York, NY, 1989 269.

[11] A. Mazahery, M.O. Shabani, Influence of the hard coated B_4C particulates on wear resistance of Al–Cu alloys, Composites: Part B 43 (2012) 1302–1308.

[12] S.K. Rhee, Wetting of AlN and TiC by liquid Ag and liquid Cu, Journal of the American Ceramic Society 53 (1970) 386.

[13] M.O. Shabani, A. Mazahery, Prediction performance of various numerical model training algorithms in solidification process of A356 matrix composites, Indian Journal of Engineering & Materials Sciences 19 (2012) 129–134.

[14] M.O. Shabani, A. Mazahery, Fabrication of AMCs by spray forming: setting of cognition and social parameters to accelerate the convergence in optimization of spray forming process, Ceramics International (2012) (12.028).

[15] G.A. Irons, K. Owusu-Boahen, Settling and clustering of silicon carbide particles in aluminum metal matrix composites, Metallurgical and Materials Transactions 26 (1995) 980–981B 26 (1995) 980–981.

[16] M.O. Shabani, A. Mazahery, The GA optimization performance in the microstructure and mechanical properties of MMNCs, Transactions of the Indian Institute of Metals 65 (1) (2012) 77–83.

[17] M. Gupta, L. Lu, S.E. Ang, Effect of microstructural features on the aging behavior of Al–Cu/SiC metal matrix composites processed using casting and rheocasting routes, Journal of Materials Science 32 (1997) 1261–1267.

[18] P.A. Karnezis, G. Durrant, B. Cantor, Characterization of reinforcement distribution in cast Al-alloy/SiC composites, Materials Characterization 40 (1998) 97–109.

[19] A. Mazahery, M.O. Shabani, Study on microstructure and abrasive wear behavior of sintered Al matrix composites, Ceramics International 38 (5) (2012) 4263–4269.

[20] C.J. Quaak, W.H. Kool, Properties of semisolid aluminum matrix composites, Materials Science and Engineering: A 188 (1994) 277–282.

[21] M.O. Shabani, A. Mazahery, Prediction of mechanical properties of cast A356 alloy as a function of microstructure and cooling rate, Archives of Metallurgy and Materials 56 (3) (2011) 671–675.

[22] A.J. Asthana, Reinforced cast metals, Part II: evolution of the interface, Journal of Material Science and Engineering 35 (1998) 1959–1980.

[23] C.A. Leon, R.L. Drew, Preparation of nickel-coated powders as precursors to reinforced metal matrix composites, Journal of Materials Science 35 (2000) 4763–4768.

[24] A. Mazahery, M.O. Shabani, Mechanical properties of squeeze-cast A356 composites reinforced with B_4C particulates, Journal of Materials Engineering and Performance 21 (2) (2012) 247–252.

[25] L.M. Tham, M. Gupta, L. Cheng, Effect of limited matrix-reinforcement interfacial reaction on enhancing the mechanical properties of aluminum–silicon carbide composites, Acta Materialia 49 (2001) 3243–3253.

[26] M.O. Shabani, A. Mazahery, Application of GA to optimize the process conditions of Al matrix nano-composites, Composites: Part B 45 (2013) 185–191.

[27] S.K. Thakur, B.K. Dhinan, The influence of interfacial characteristics between SiCp and Mg/Al metal matrix on wear, coefficient of friction and microhardness, Wear 247 (2001) 201.

[28] S.F. Moustafa, S.A.L. Badry, A.M. Sanad, B. Kieback, Friction and wear behavior of graphite–copper composites, Wear 253 (2002) 699–710.

[29] A. Mazahery, M.O. Shabani, A comparative study on abrasive wear behavior of semisolid–liquid processed Al–Si matrix reinforced with coated B_4C reinforcement, Transactions of the Indian Institute of Metals 65 (2) (2012) 145–154.

[30] U. Cocen, K. Onel, Ductility and strength extruded aluminum alloy composites, Composite Science Technology 62 (2002) 275–282.

[31] M. McKimpson, T. Scott, Processing and properties of metal matrix composites containing discontinuous reinforcement, Materials Science and Engineering 107 (1989) 93–106.

[32] A. Mazahery, M.O. Shabani, The accuracy of various training algorithms in tribological behavior modeling of A356-B_4C composites, Russian Metallurgy (Metally) 7 (2011) 699–707.

[33] J. Kennedy, R. Mendes, Population structure and particle swarm performance, in: Proceedings of the IEEE World Congress on Evolutionary Computation, Honolulu, Hawaii, May 2002, 1671–1676.

[34] P. Sathiya, S. Aravindan, A.N. Haq, K. Paneerselvam, Optimization of friction welding parameters using evolutionary computational techniques, Journal of Materials Processing Technology 209 (2009) 2576–2584.

[35] J.J. Liang, A.K. Qin, P.N. Suganthan, S. Baskar, Comprehensive learning particle swarm optimizer for global optimization of multimodal functions, IEEE Transactions on Evolutionary Computation 10 (2006) 281–295.

[36] M.O. Shabani, A. Mazahery, The ANN application in FEM modeling of mechanical properties of Al–Si alloy, Applied Mathematical Modelling 35 (2011) 5707–5713.

[37] J. Kennedy, R.C. Eberhart, Particle swarm optimization, in: Proceedings of the IEEE International Conference on Neural Networks IV, Perth, Australia, 1995, 1942–1948.

[38] A.P. Engelbrecht, B.S. Masiye, G. Pampara, Niching ability of basic particle swarm optimization algorithms, in: Proceedings of the IEEE Swarm Intelligence Symposium, 2005.
[39] A. Mazahery, M.O. Shabani, Process conditions optimization in Al–Cu alloys matrix composites, Powder Technology 225 (2012) 101–106.
[40] R.A. Krohling, E. Mendel, Bare bones particle swarm optimization with Gaussian or Cauchy jumps, in: Proceedings of the IEEE Congress on Evolutionary Computation, CEC'09, 2009 3285–3291.
[41] M.O. Shabani, A. Mazahery, Artificial Intelligence in numerical modeling of nano sized ceramic particulates reinforced metal matrix composites, Applied Mathematical Modelling 36 (2012) 5455–5465.
[42] D. Beasley, D.R. Bull, R.R. Martin, A sequential niching technique for multimodal function optimization, Evolutionary Computation 1 (2) (1993) 101–125.
[43] R. Brits, Niching strategies for particle swarm optimization, Master's thesis, Department of Computer Science, University of Pretoria, Pretoria, South Africa (2002).
[44] M.O. Shabani, A. Mazahery, Application of FEM and ANN in characterization of Al matrix nano composites using various training algorithms, Metallurgical and Materials Transactions A 43 (2012) 2158–2165.
[45] J. Kennedy, Small worlds and mega-minds: effects of neighborhood topology on particle swarm performance, in: Proceedings of the IEEE Congress on Evolutionary Computation, July 1999 1931–1938.
[46] A. Mazahery, M.O. Shabani, A356 reinforced with nano particles: numerical analysis of mechanical properties, JOM 64 (2) (2012) 323–329.
[47] M.O. Shabani, A. Mazahery, Aluminum-matrix nanocomposites: swarm-intelligence optimization of the microstructure and mechanical properties, Materiali in tehnologije 46 (6) (2012) 613–619.
[48] F. van den Bergh, A.P. Engelbrecht, A study of particle swarm optimization particle trajectories, Information Science 176 (8) (2006) 937–971.
[49] M.O. Shabani, A. Mazahery, Microstructural prediction of cast A356 alloy as a function of cooling rate, JOM 63 (8) (2011) 132–136.
[50] Y.G. Petalas, C.G. Antonopoulos, T.C. Bountis, M.N. Vrahatis, Detecting resonances in conservative maps using evolutionary algorithms, Physics Letters A 373 (2009) 334–341.
[51] A. Mazahery, M.O. Shabani, Assistance of novel artificial intelligence in optimization of aluminum matrix nanocomposite by genetic algorithm, Metallurgical and Materials Transactions A 43 (2012) 5279–5285.
[52] C.H. Wu, N. Dong, W.H. Ip, C.Y. Chen, K.L. Yung, Z.Q. Chen, Chaotic hybrid algorithm and its application in circle detection, Lecture Notes in Computer Science 6024 (2010) 302–311.
[53] M.O. Shabani, M. Alizadeh, A. Mazahery, Modelling of mechanical properties of cast A356 alloy, Fatigue and Fracture of Engineering Materials and Structures 34 (2011) 1035–1040.
[54] S.Z. Zhao, P.N. Suganthan, Two-lbests based multi-objective particle swarm optimizer, Engineering Optimization 43 (1) (2011) 1–17.